Erosion Wear Behavior of Inconel625 Plasma Transferred Arc Weld (PTAW) Deposits using Air Jet Erosion Tester

[1]Abhishek Jivrag, [2]Shashikant Pople

ABSTRACT

This paper studies the effect of Inconel625 as wear resistant material to control erosion wear. The work attains to establish the mechanisms of erosion wear on Inconel625, by considering impacting angles of particles at different temperature of Inconel625 substrate as process parameters and wear rate as response parameter. Fractional Factorial Regression method is used for developing relationship between process parameters and response parameter. The adequacy of model is tested by ANOVA. The Inconel625 material is developed through Plasma Transfer Arc Welding (PTAW) Technique and the tests are conducted according to ASTM G-76 Standards on Air Jet Erosion Test Rig.

Keywords: **Erosion Wear, Inconel625, PTAW, ASTM G-76 Standards, Full Factorial Regression Design & ANOVA**

I. INTRODUCTION

Wear is defined as removal of material from target surface due to relative motion between the target surface and any of the three different states of matter [4],[5]. Erosion wear is amongst the principle forms of wear, caused by the impingement of solid particle, streams of liquid and gases on target surface, leading towards material abstraction [4]. It is observed in transfer of solids, fluids and gases through channels and pipeline, valves, valve seats of I.C engines, parts of nuclear plants and chemical plants, accessories of ships and aero-planes etc.

Parameters affecting solid particle erosion include-impact angle, impact velocity, solid particle material, particle shape and size, carrier fluid, class of target material, state of material, environmental conditions etc. *Wear is not a material property; it is a system response* [4]. Different models explaining erosion wear mechanisms have been devised by Finne [1], and Bitter [2],[3]. Catastrophic failure of components does not occur at once and all of a sudden as wear acts in stages.

[1]Abhishek Jivrag is presently pursuing his bachelor's degree in mechanical engineering from MGM's Jawaharlal Nehru Engineering College, N-6 CIDCO, Aurangabad, Maharashtra, India (Contact no.: +919422229096 email: abhishek.jivrag@gmail.com)

[2]Shashikant Pople is currently a final year student of electronics and telecommunication engineering at MGM's Jawaharlal Nehru Engineering College, N-6 CIDCO, Aurangabad, Maharashtra, India (Contact no.: +919423734224 email: shashikantpople16@gmail.com)

II. LITERATURE SURVEY

Cobalt base alloys namely stellite-6 & stellite-12 having excellent resistance to wear and corrosion, are used for hard facing of different components. In nuclear components use of Co_{60} alloys, leads to induced activity from transmuted Cobalt isotope formed in nuclear reactive environment [7]. Nickel base alloys are a new class of materials which do not lead to induced activity in nuclear plants and have gained importance in controlling wear phenomena. The properties of Colmonoy6 have been studied in this regard [7]. Inconel625 is also a nickel base alloy, constituting Nickel-58%, Chromium 20-23% Molybdenum 8-10%, Iron 5%, Niobium and Tantalum 3-4%. Elements such as Carbon, Titanium, silicon, manganese, aluminium are present in trace amounts. It bears the properties of wear and corrosion resistant materials.

Hence erosion wear behavior of Inconel625 would furnish important data; making its use prominent, in protecting various components from erosion wear.
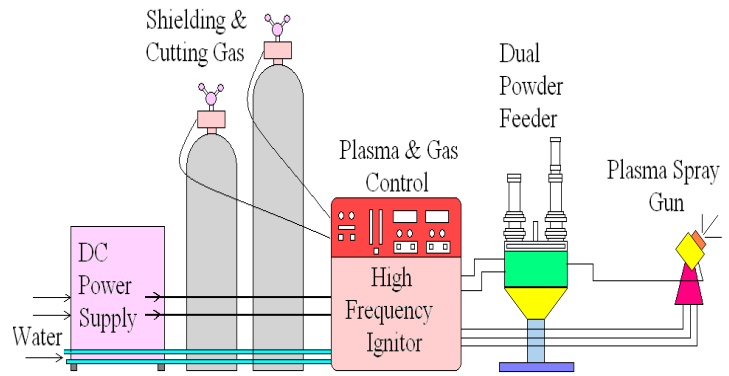
III. EXPERIMENTAL

A. Development of Inconel625 deposits using PTAW

Plasma arc transfer welding is a process, in which the joining of materials is produced by the heat of constricted arc between an electrode and base metal. In plasma arc welding, a shielded arc is struck between a non consumable electrode (Tungsten) and the torch body, and this arc transforms an inert gas into plasma by heating it to a high temperature [8]. The plasma arc welding process uses this plasma to transfer an electric arc to a work piece. Inconel625 powder is melted by the intense heat of the arc in the plasma torch which fuses it to base substrate with low dilution. Plasma is a distinct state of matter in which a certain proportion of electrons are free than being bounded to an atom or molecule. The ability of the positive and negative charges to move independently makes the plasma electrically conductive.

Austenitic Steel 316L SS acts as a substrate for developing Inconel625 deposits. The deposited substrate obtained after cooling, is ground to fine surface finish and cut into subparts to specimen dimensions as stated in ASTM G-76 standards.

Table I: ASTM G-76 Standard specification for solid particle erosion wear

S.No	Particulars	Standard Specification
01.	Nozzle Inner Diameter (mm)	1.5 ± 0.075
02.	Nozzle Length (mm)	50
03.	Test Gas	Dry Air
04.	Lower point of test gas (°C)	-50
05.	Abrasive Particle	Al_2O_3
06.	Particle size (µm)	50
07.	Particle velocity (m/s)	30 ± 2
08.	Gas Flow Rate(l/min)	8
09.	System Pressure(GPa)	140
10.	Steady state condition time(s)	10
11.	Size of erosion (mm deeper)	1
12.	Temperature of ambience(°C)	18 – 28
13.	Particle feed rate(gm/min)	2 ± 0.5
14.	Particle Flux(mg/mm^{2}s)	2
15.	Working Distance (mm)	10 ± 1
16.	Specimen Rectangular size(mm x mm x mm)	10 x 30 x 2
17.	Reference Specimen	Type 1020 Steel
18.	Performance verification	After every 50 tests
19.	Nozzle diameter material	WC, Al_2O_3
20.	Specimen surface Roughness(µm)	1

Table II: Wear Rate values for various parametric combination

S.No	Temperature (T) °C	Impact Angle (θ) °(Degree)	Wear Rate (WR) gm/min
01.	30	30	0.0494
02.	30	90	0.0180
03.	200	30	0.0556
04.	200	90	0.0185
05.	30	60	0.0254
06.	30	60	0.0256

Table III: Analysis of Variance (ANOVA) for Erosion Wear (coded units)

Source	DF	Seq SS	Adj SS	Adj MS	F	P
Main Effects	2	0.0012 4707	0.001 24707	0.0006 2353	18. 54	0.0 51
2-Way Interactions	1	0.0000 0812	0.000 00812	0.0000 0812	0.2 4	0.6 72
Residual Error	2	0.0000 6726	0.000 06726	0.0000 3363		
Lack of Fit	1	0.0000 6724	0.000 06724	0.0000 6724	3E +03	0.0 11
Pure Error	1	0.0000 0002	0.000 00002	0.0000 0002		
Total	5	0.00132245				

DF- Degrees of Freedom   SS-Sum of squares
MS- Mean Square   F- Fisher Value
P- Probability Value   Adj- Adjusted

Fig 1: Plasma Transfer Arc Welding System

B. Erosion Wear Test

The erosion wear tests were performed according to specifications stated in ASTM G-76 standards (Table I).

The experiments are performed in air jet erosion test rig [9]. Full Factorial regression method is incorporated to draw relation between process and response parameters. Temperature and impact angles are considered as process parameters whereas wear rate is considered as response parameters. Process parameters such as standoff distance, pressure, cycle time etc. have specific values in ASTM G-76 standards and are set with the help of digital control panel sited on the test rig [9].

IV. RESULTS

The experiments are conducted at temperature of 30°C and 200°C by taking impact angle viz. 30°, 60°and 90°as process parameters. Wear rates for different parametric combinations of temperature and impact angles are calculated by subtracting the weight before and after performing erosion wear test (Table II).

Erosion wear rate (gm/min)
= [Weight before wear test – Weight after wear test]

All observations taken at 30°C are on a single sample. Similarly observations for 200°C are also on same sample, so that the target surface crystallographic structural characteristics for different parameters remain legitimate. Experiments are performed on Inconel625, in air jet erosion test rig, according to ASTM G-76 standards.

In applying full factorial design [13], temperature of 30°C and impact angle of 60°are taken as intermediate value to check repeatability.

ANOVA Test (ANalysis Of VArience): These tests are carried out in order to determine the most significant factor present in the experiment in context to others (Table III). The importance of this test is to give a mathematical equation to the values (Table IV) obtained from the present reading; maintaining precision for error between practical values and the theoretical values that will be obtained from the equation.

Table IV: Estimated Coefficients for Wear using data in uncoded units

| Term	Coefficient
Constant	0.0586794
Temperature	0.0000773529
Impact Angle	-0.000506569
(Temperature) x (Impact Angle)	-5.58824E-07

The relation deduced by full factorial regression method is:

W.R. = 0.0586+0.0001T-0.0005θ -5.588 T θ
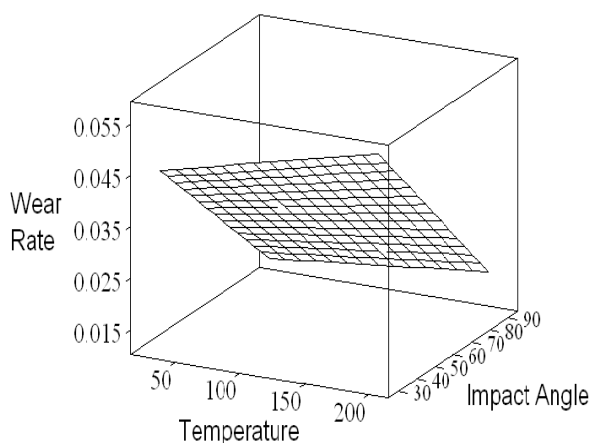
Fig 2: 3-D Model developed by Full Factorial   Regression Method

V. CHARACTERIZATION

The abrasive particles impinge the target surface with an impact force which can be resolved into two components. Horizontal component of impacting force results in cutting action and vertical component of impact force results in plastic deformation [10].
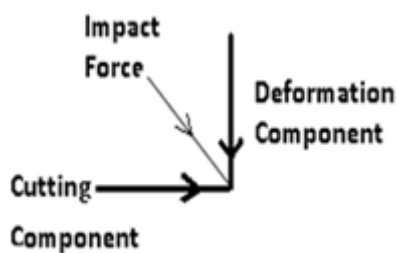

Fig 3: Components of impact force i.e. deforming and cutting action of particle on target surface

Cutting component of impact force dominates at shallow angles of impact while deformation component plays major role at larger impacting angles. When the particles having kinetic energy hit the target surface, transformation of energy to the surface is observable in form of elastic and plastic deformation. Initially elastic deformation builds up stress concentration at contact points. An increase of elastic limit above the strength of material induces plastic deformation. Small cracks are induced as the value of shear deformation increases than the shear strength of material. The cracks then nucleate and propagate progressively. The cutting action of horizontal component ploughs and shears the target surface causing removal of material.
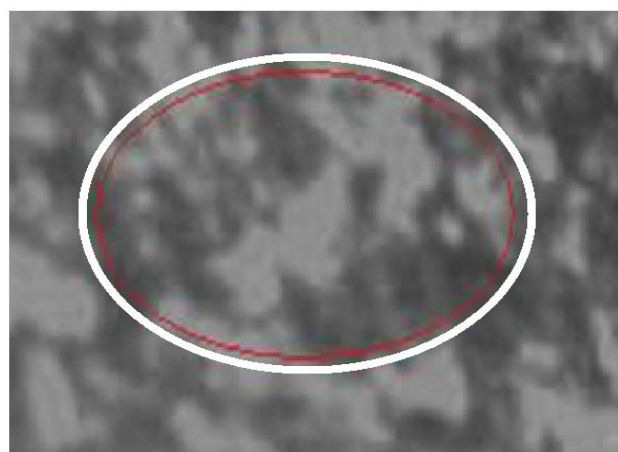
A. Target Surface Impinged at an Impact angle of 60˚
Fig. 5, depicts the surface essentially impinged by particles, which are conical or diamond shaped. The cutting component and deformation components of impact force plays equal role in material abstraction. The particles also revolve while impinging on the substrate. Hence after the removal of material from one of the vertex of the particle, the momentum associated with it tries to revolve the particle, bringing the next vertex point in contact with the target surface and removes the material in a similar fashion (Fig. 4) but with reduced intensity, as particle transfers a significant amount of energy to the target surface during primary impingement. The rotation of particle to cause removal of material decreases with successive impacts.
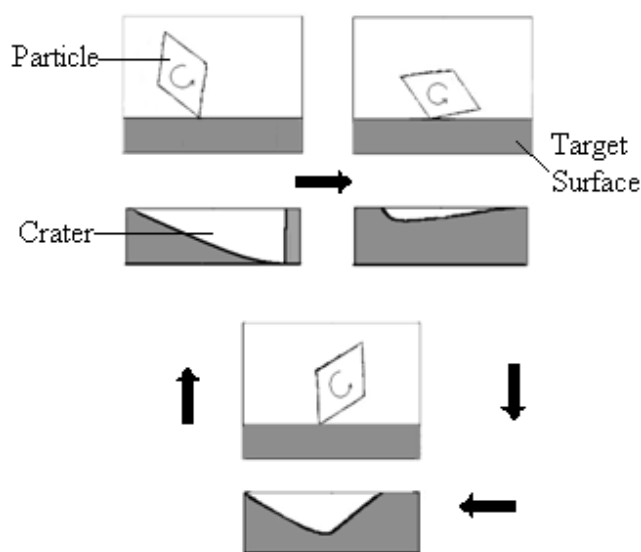
Fig 4: Successive removal of material from different vertices impacting particle

At steep impact angle of 60° the tunneling effect or ploughing effect is responsible for giving deep slanted circular shape to the eroded area. The tunneling effect can be observed in Fig. 5, as the white patch which signifies target surface, appears raised. The forward rotating particle piles up the removed material more than the backward

Figure 5: Photograph substantiating the effect of wear at impact angle of 60°

rotation of particles[11]. It can be seen from Fig. 8 that backward rotation of particles takes place as less piling of material is observed.

B. Target Surface Impinged at an Impact angle of 30•

The particles also remove the material in a similar fashion by deformation & cutting action. Fig 6 shows that, primary impacts create some circular and irregular shaped holes primarily due to sudden collision of varying sized particles, transferring energy and the secondary impacts leads to a weathered surface due to decreasing intensity to remove material.

The weathered surface depicts that cutting component of impacting force dominates over deformation wear as observed in Fig. 6.
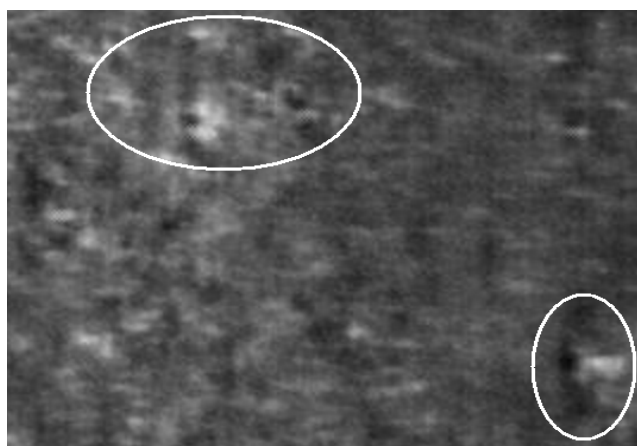

Fig. 6: Photograph showing wear at an inclination 30˚. Circles depict the primary impact while non circled area is the withered target surface due to secondary impacts of particles

Thus the overall effect of impingement of particles on the target surface is mild as there is less penetration of particles (Fig. 6) at impact point due to shallow impingement angle. Also the revolving velocity of the particle gradually reduces as sudden impacts of particles do not occur [8]. Hence material removal occurs progressively as vertices of the particle, impact the target surface repeatedly due to gradually reducing momentum retained in them, after successive impacts.

Material removed at both; primary and secondary impacted surfaces, adds to the total material detached from the surface. Thus the wear removal rate is maximum in this case.

The crater formation occurring at 30° impingement of particles is essentially oval in shape and slanted towards the sharper end (Fig.8). This can be credited to the backward rotation of particle eroding the surface area at shallow lengths. The plastic deformation causes piling of material at one corner giving sharper oval curve at one end. The jet of abrasive material has acquired a cylindrical shape due to its travel through the internal bore of the nozzle. The base of the cylindrical erodent particle jet on the target surface

acquires slanted shape, and not perfectly circular as compared to that of the nozzle opening.

C. Target Surface Impinged at an Impact angle of 90•

In this case, the plastic deformation is the dominant factor [11]. The particles at first, elastically and then plastically deform the surface. The surface is then subjected to shear deformation which induces cracks into the surface and the particles finally rupture the surface thereby piercing through it. During impingement, the particles transfer a major portion of kinetic energy and get stuck on the target surface, which leads to limited secondary impacts.

Fig. 7: Photograph of particle impinging normally to target surface

As a consequence of rupture, a built up edge or lip formation at the crater edge takes place. It is due to the neighboring impact of particles which imposes repeated cycles of plastic deformation that leads to accumulation of plastic strain [14]. When this value of plastic strain reaches above the critical value of strain of the target surface, the piled up material in the vicinity of the crater is removed and the particle is removed due to the spring back effect. The shape of the eroded area on target surface essentially appears to be circular (Fig.8). This can be attributed to the fact that the abrasive particles base acquires circular shape due to its passage through cylindrical nozzle. The wear rate is smaller as the cutting component leading to shearing of material plays a minor role.
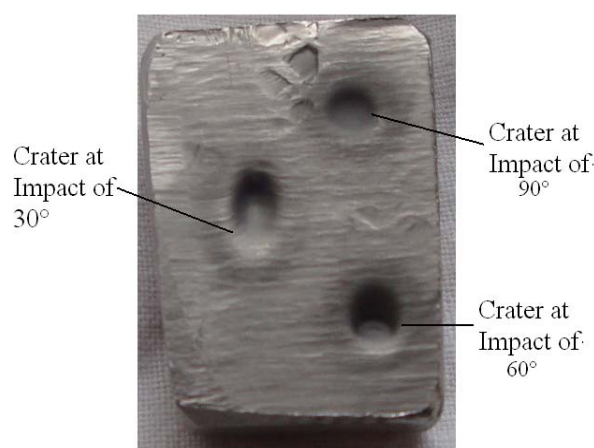

Fig 8: Photograph of target surface Inconel625 after erosion wear test at different impact angle at 30˚C

VI. CONCLUSIONS

1. The wear rate is maximum at 30°, sharply decreases at 60° and is minimum at 90°. Thus rate of wear goes on decreasing from 30° to 90°. This provides the evidence that Inconel625 despite having hardness value around 350 VHN follows the wear trend of ductile material and not of hard material as expected from its hardness value.

2. The wear rates observed at 30°C and 200°C, show a negligible change in their reading thus illustrating that Inconel-625 coated components can be used at 200°C without significant material loss.

3. The depth of intruding target surface is higher for impact angle of 90° and goes on decreasing at 60° and 30°. This is because cutting wear plays a minor role during 90° impingement. Deformation component is solely responsible for penetrating depth in target surface.

4. At shallow impact angles, it is the cutting wear which predominates over deformation wear, which accounts for increase of wear rate. The component of cutting force shears the target surface over larger lengths at 30° than compared to 60°.

5. The particles come to rest on the target surface for larger angle of attack. At lower angles (i.e. at 30°), backward spinning of particles occur, due to ingrained momentum restored after successive impacts, as transfer of kinetic energy does not occur all of a sudden due to smaller depths of invasion.

REFERENCES

[1] Finne, I., Erosion of surfaces by solid particles, Wear, Vol. 3, PP 87 (1960)

[2] Bitter, J.G.A, A study of erosion phenomena part I, Wear, Vol. 6, PP 5 (1963)

[3] Bitter, J.G.A, A study of erosion phenomena part II, Wear, Vol. 6, PP 169 (1963)

[4] Bharat Bhushan, Modern Tribology Handbook, PP 273-312, CRC Press LLC (2000).

[5] Gupta, B.K. and Bharat Bhushan, Handbook of tribology-Materials, Coatings & Surface Treatments,Vol-I , PP 2.1-2.68, Mc Graw Hills (1991)

[6] Bitter, J.G.A , A study of erosion wear phenomena Part I and II, Koninklijkel Shell-Laboratorium, Shell International Research, PP 1-40 (1962)

[7] Gurumoorthy, K., M. Kamaraj, K. Prasad Rao, A. Sambasiva Rao, S. Venugopal, Micro structural aspects of plasma transferred arc surfaced Ni-based hardfacing alloy, Materials Science and Engineering: A, Vol. 456, Issues 1-2, , PP 11-19(2007)

[8] Zielińska, S., F. Valensi, N. Pellerin, *et al.*, Microstructural analysis of the anode in gas metal arc welding (GMAW), Journal of Materials Processing Technology, Vol. 209, Issue 7, , PP 3581-3591 (2009)

[9] Magnum Engineers, Manual of Air Jet Erosion Test Rig, PP 01-35, Banglore (2009)

[10] Dhar, S., T. Krajac, D. Ciampini, M.Papini, Erosion mechanism due to impact of single angular particle, Wear, Vol. 258, Issues 1-4, , PP 567-579 (2005)

[11] Dundar, M. and O.T. Inal, Solid particle erosion of a-brass with 5 and 25 mm particles at normal incidence, *Wear, Vol. 224, Issue 2, , PP 226-235 (1999)*

[12] Oka, Y.I., H. Ohnogi, T. Hosokawa, M. Matsumura, The impact angle dependence of erosion damage caused by solid particle impact, Wear, Vol. 203-204, PP 573-579 (1997)

[13] Benyounis, K.Y. and A.G. Olabi, Optimization of different welding processes using statistical and numerical approaches – A reference guide Advances in Engineering Software, Vol. 39, Issue 6, PP 483-496 (2008)

[14] Papini, M. and J.K. Spelt, Impact of rigid angular particles with fully-plastic targets Part II: Parametric study of erosion phenomena, International Journal of Mechanical Sciences, Vol. 42, PP 1007-1025 (2000)